Water and chloride as allosteric inhibitors in WNK kinase osmosensing

Liliana R. Teixeira[a], Radha Akella[a], John M. Humphreys[a], Haixia He[a], Elizabeth J. Goldsmith[a]

[a] Department of Biophysics, The University of Texas Southwestern Medical Center, 5323 Harry Hines Boulevard, Dallas, TX 75390-8816, USA

KEYWORDS: WNK, kinase, water, allostery, autophosphorylation, osmosensing, WNK1, WNK3, crystallography, mass spectrometry

ABSTRACT

Previous observations showed that chloride and osmotic stress regulate the autophosphorylation and activity of the kinase domains of WNK1 and WNK3. Further, prior crystallography on the asymmetric dimeric of the unphosphorylated WNK1 kinase domain (WNK1/S382A, WNK1/SA) revealed conserved waters in the active site. Here we show by crystallography that PEG400 applied to crystals of dimeric WNK1/SA grown in space group P1 induces de-dimerization with a change in space group to $P2_1$. Both the conserved waters, referred to here as conserved water network 1 (CWN1) and the chloride binding site are disrupted by PEG400. CWN1 is surrounded and stabilized by a pan-WNK-conserved cluster of charged residues. Here we mutagenized these charges in WNK3 to probe the importance of the CWN1 to WNK regulation. Two mutations at E314 in the Activation Loop (WNK3/E314Q and WNK3/E314A) enhanced activity, consistent with the idea that the CWN1 is inhibitory. Mutations of other residues in the cluster had similar or less activity than wild-type. PEG400 activation of WNK3 was not significantly reduced in the point mutants tested. The crystallographic and assay data support a role for CWN1 and the charged cluster in stabilizing an inactive configuration of WNKs and suggest that water functions as an allosteric inhibitor of WNKs.

INTRODUCTION

With No Lysine (WNK) kinases are soluble intracelluar serine-threonine kinases noted for their unique active site (Xu *et al*, 2000) and their association with familial hyperkalemic hypertension (FHHt) (Wilson *et al*, 2001). Previous data has implicated WNKs as homeostatic regulators of the intracellular milieu with respect to ions and osmotic pressure (reviewed in (Goldsmith & Rodan, 2023; Richardson & Alessi, 2008)). WNKs are the chloride-inhibited protein kinases long anticipated from cellular studies to control the activity of cation chloride cotransporters in response to osmotic stress (Lytle & Forbush, 1992). WNKs are activated by osmotic stress in cells (Xu *et al.*, 2000). We demonstrated that WNKs 1 and 3 are inhibited by chloride (Piala *et al*, 2014) and are directly activated *in vitro* by osmolytes (Akella *et al*, 2021).

Previous data has shown that unphosphorylated WNK1 and WNK3 adopt an asymmetric dimer configuration (Akella *et al.*, 2021; Min *et al*, 2004), data acquired either using non-phosphorylatable WNK1/SA, or de-phosphorylated WNK1 and WNK3 kinase domains (uWNK1 and uWNK3, "u" for unphosphorylated). Phosphorylated kinase domains of WNK1 and WNK3 (pWNK1 and pWNK3, "p" for phosphorylated) are monomeric (Akella *et al*, 2020) (PDB files 5W7T and 5O26). Chloride ion is a pan-WNK inhibitor (Piala *et al.*, 2014; Terker *et al*, 2016) and binds the inactive dimer (Piala *et al.*, 2014). Osmotic pressure was applied using osmolytes to put a demand on solvent in vitro (Kuznetsova *et al*, 2014). Osmolytes induced de-dimerization as observed by SLS and SAXS in both uWNK1 and uWNK3 (Akella *et al.*, 2021). A model for WNK regulation, then, is the presence of a dimer⇔monomer equilibrium: the dimer is inactive and binds inhibitory ligands; the monomer is autophosphorylation-competent. We described previously that the inactive dimer, counter-intuitively, has more bound water than the monomeric form in bulk (Akella *et al.*, 2021). We also identified a large network of water molecules that is

independently observed in two WNK1/SA structures (PDB files 6CN9 and 5DRB (Yamada *et al*, 2016)). Here we refer to this water network as Conserved Water Network 1 (CWN1, Figure 1A).

Here we present crystallographic data that the osmolyte PEG400, when applied to crystals of WNK1/SA, induces de-dimerization (forming monomers) and conformational changes. Comparison of the water structure in the inactive dimer versus the PEG400-induced conformation supports the idea that water is an allosteric ligand binding an inactive WNK configuration, and that an osmolyte-induced demand on solvent favors a structure with less bound water, overall and in water networks.

We further present a mutagenic study. A pan-WNK conserved cluster of charged residues surround and stabilize the water network CWN1 (Akella *et al.*, 2021). This amino acid cluster is between the Activation Loop and Catalytic Loop (referred to here as the AL-CL Cluster). Here we analyze the effect of mutating the AL-CL Cluster on WNK activity and regulation. The mutagenic study was carried out primarily on WNK3, the kinase domain most sensitive to osmotic pressure among WNK kinase domains tested. In this study, we observe both positive and negative effects of mutations on WNK3 activity and regulation.

RESULTS

Conserved Water Networks in WNKs.

CWN1 in WNK1/SA, and by extension other unphosphorylated WNKs is a salient feature both in 6CN9 and 5DRB. ProBis-H2O (Jukic *et al*, 2020) was used to find water clusters across WNK1 structures, then curated in PyMOL (see Methods). Two water clusters were identified (CWN2 and CWN3) in addition to CWN1 (Figure 1B). Of the 14 waters that

make up CWN1 in PDB file 6CN9, nine are conserved in PDB file 5DRB (Figure 1C (5DRB waters are yellow)). 5DRB has two non-identical waters in this region. Another network of waters, CWN2, was found by superimposing the N-terminal domains of 6CN9 and 5DRB. CWN2 is in the subunit interface in 6CN9 which is a lattice contact in 5DRB (Figure 1D). Another set of eight conserved waters (CWN3, Figure 1B) is present near helix E. These waters are also observed in phosphorylated WNK1 (PDB file 5W7T).

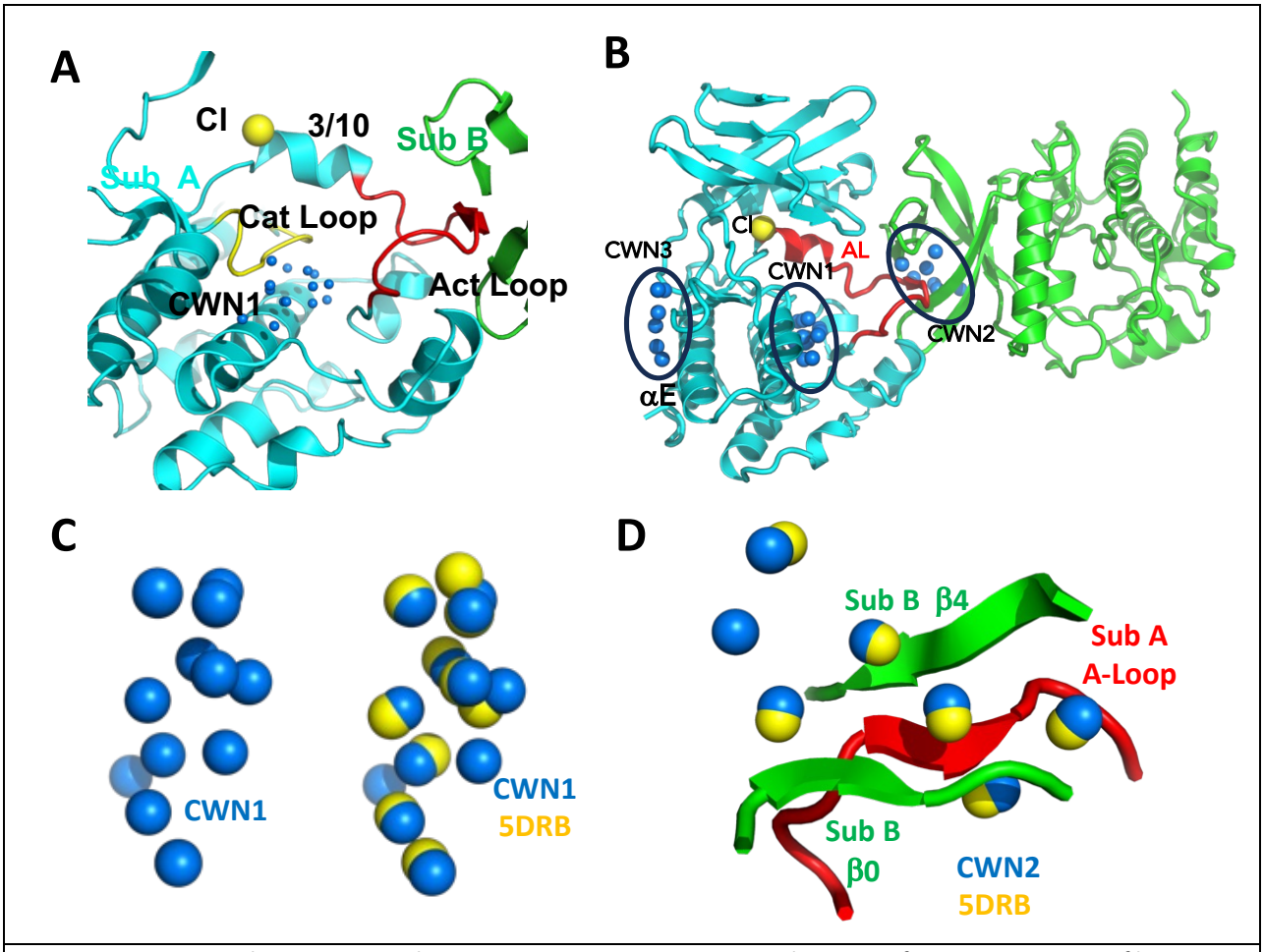

Figure 1. Conserved water networks in WNK1/SA. (A) CWN1 in Subunit A of uWNK1/SA (PDB file 6CN9). Conserved water network 1 (CWN1) in marine, 14 water molecules. Subunit A, cyan, Subunit B, green, Activation Loop, red, and Catalytic loop, yellow. (B) Three observed water networks (CWN1-3, black ovals) were identified by superposition of PDB 6CN9 and 5DRB. Colors are as in (A). (C) Overlay of waters in PDB files 6CN9 (marine) and 5DRB (yellow). (D) CWN2 is in the subunit interface (same coloring as in (A). N-terminal domains were superimposed.

PEG400 disrupts the water networks CWN1 and CWN2 and the chloride binding site.

Crystals grown in PEG3350 and potassium formate are similar in structure to the previously reported WNK1/SA, (PDB file 6CN9) exhibiting an asymmetric dimer and the same water clusters as 6CN9. Two different reagents were used for cryoprotection, glycerol and PEG400. Crystallographic data collection parameters and

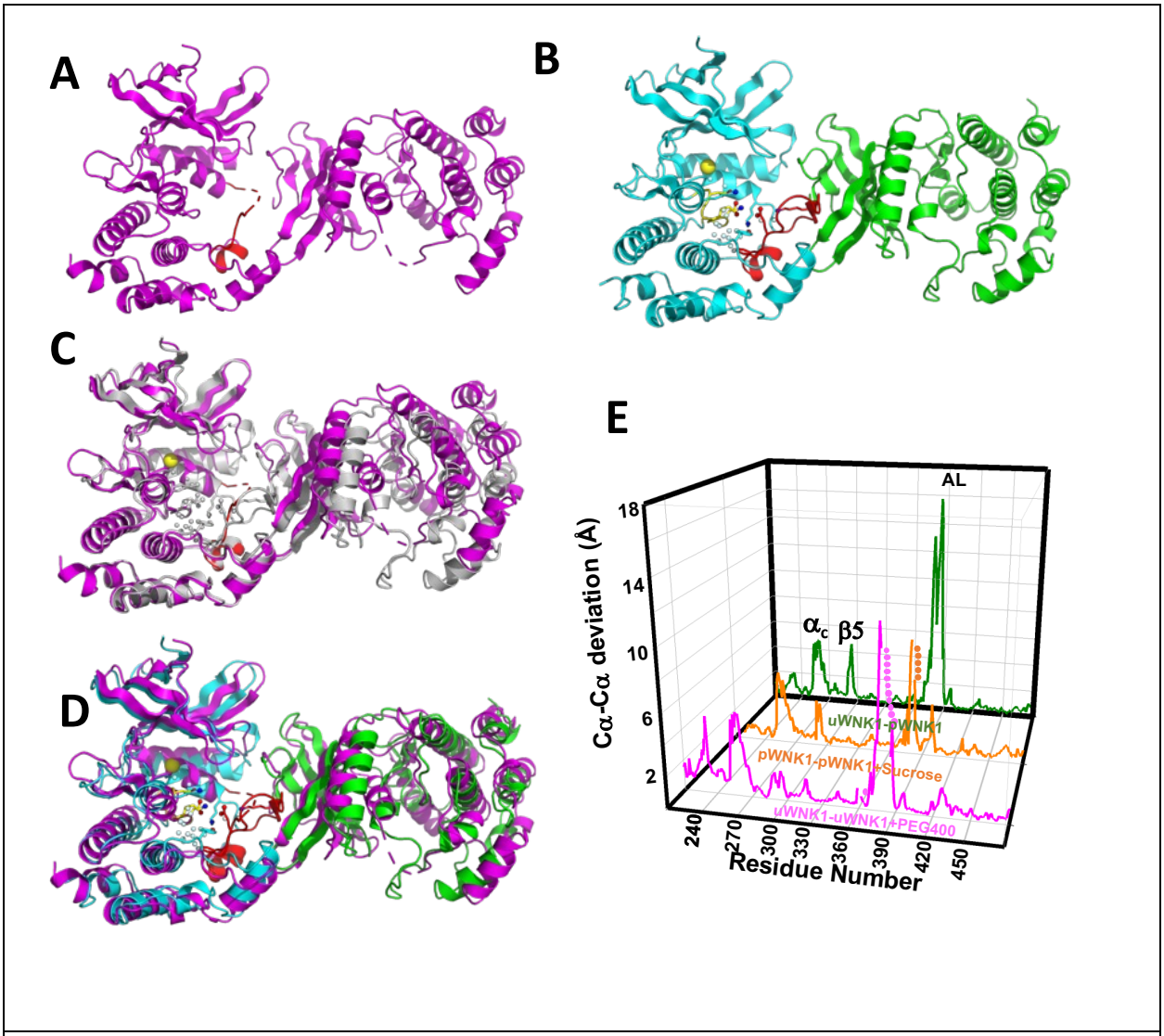

Figure 2. Effects of PEG400 on the WNK1/SA dimer and space group. Monoclininc WNK1/SA/PEG400 (PDB in submission) with symmetry mate (pink) (A) and WNK1/SA (PDB 6CN9) (B) are superimposed (6CN9 in grey) (C). (D) Superposition of one subunit of WNK1/SA/PEG400 from (A) with WNK1/SA from (B) to show rotation that accompanies monomer conversion induced by PEG400. (E) Osmolyte induced conformational changes as a function of sequence. WNK1/SA (PDB file 6CN9) and WNK1/SA/PEG400, pink trace, pWNK1 (PDB 5W7T) and pWNK1/sucrose (Akella *et al.*, 2020), orange trace, and pWNK1 and PKA (PDB file 1ATP), green trace.

refinement statistics of the two structures are given in Table S1. The structure observed in glycerol-soaked crystals was very similar to the previously determined 6CN9. On the other hand, PEG400-soaked crystals revealed a significantly altered structure (Table S2). PEG400 induced a space group change from P1 to $P2_1$ (cell constants compared in Table S2) (see Methods). WNK1/SA cryoprotected in glycerol is dimeric. In the presence of PEG400, WNK1/SA monomerizes in the crystal (lattice constants are compared in Table S2). We observed previously that the osmolyte ethylene glycol induces a dimer-to-monomer transition in solution (Akella *et al.*, 2021)). The change in structure induced by PEG400 is illustrated in Figure 2: the WNK1/SA monomer from WNK1/SA/PEG400 together with the appropriate symmetry mate (Figure 2A) is superimposed with the WNK1/SA dimer (PDB file 6CN9) (Figure 2B), as shown in Figure 2C (giving an overall r.m.s.d. of 3.2Å (Table S2). Figure 2D shows the overlay aligning one subunit to reveal a significant rotation that accompanies the monomer conversion induced by PEG400. Superpositions of monomers show that the PEG400-induced monomer is more similar to the A-chain of PDB 6CN9. The PEG-induced structure exhibits the same similarity to pWNK1 (PDB file 5W7T). Figure 2E shows the locus of conformational changes across the sequence and compares this with the osmolyte-induced changes in phosphorylated forms of WNK1. As with the effect of the osmolyte sucrose on pWNK1 (Akella *et al.*, 2020), conformational changes occur in the Activation Loop and near helix C and β5.

PEG400 affects both CWN1 and the chloride-binding 3/10 helix (Figure 3A). A prominent change in interactions occur on WNK1/K375 and WNK1/D349 (Figure 3B). PEG400 induces significant losses in the CWN1, with only 5 waters left out of the 14 in CWN1 (electron density of water molecules shown in Figure 3C). An active configuration of WNK1, pWNK1 (PDB file 5W7T) has even fewer bound waters (Figure 3D). Apparently,

the osmolyte PEG400 affects both the water and chloride binding sites of WNK1/SA. CWN2 is completely lost in PEG400.

Probing the potential role of water networks in osmosensing

We explored the role of CWN1 by mutational analysis of the AL-CL cluster. Pan-WNK conserved residues in the AL-CL Cluster are shown in Figure 4. Activation Loop residues E388, K381, and K375 of WNK1 interact with Catalytic Loop residues WNK1/D349, K351

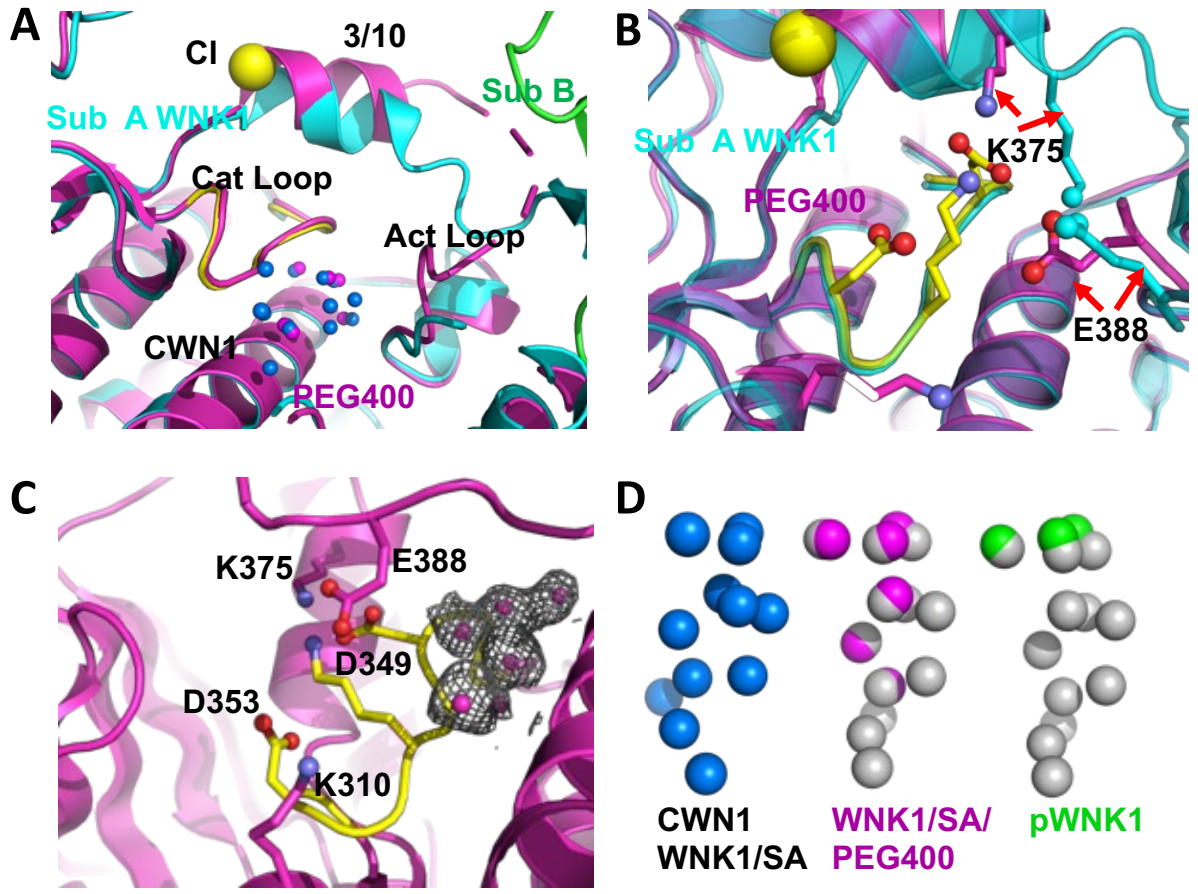

Figure 3. PEG400-induced conformational change in the active site of WNK1/SA. (A) PEG400 induced conformational changes in WNK1/SA. WNK1/SA Sub A (cyan), Sub B (green), superimposed with WNK1/SA/PEG400 (pink). (B) Conformational changes in the active site in both the 3/10 chloride binding helix and the Activation Loop, same coloring as in (A). Residues E388 and K375 move significantly (red arrows), affecting the 3/10 helix, and the CWN1 binding pocket present in WNK1/SA. (C) Electron density of waters in WNK1/SA/PEG400. (D) Overlay of CWN1 with waters remaining in PEG400 (magenta), and waters remaining in pWNK1 (PDB file 5W7T) (green).

and D353 (Figure 4A). WNK1/D349 and WNK1/K351 are pan-kinase catalytic residues. Additional residues in the active site cavity, WNK1/K310, K375, K381, and Y420, contribute to the AL-CL cluster. The AL-CL Cluster is conserved in WNK3 and other WNKs (Figure 4B). WNK1/E388 (WNK3/314) is noteworthy because it is on the Activation Loop that undergoes large conformational changes upon phosphorylation (Akella *et al.*, 2020). WNK1/D353 (WNK3/D279N) is noteworthy because it is often glutamate in other protein kinases and involved in substrate recognition (Manning *et al*, 2002; Zheng *et al*, 1993).

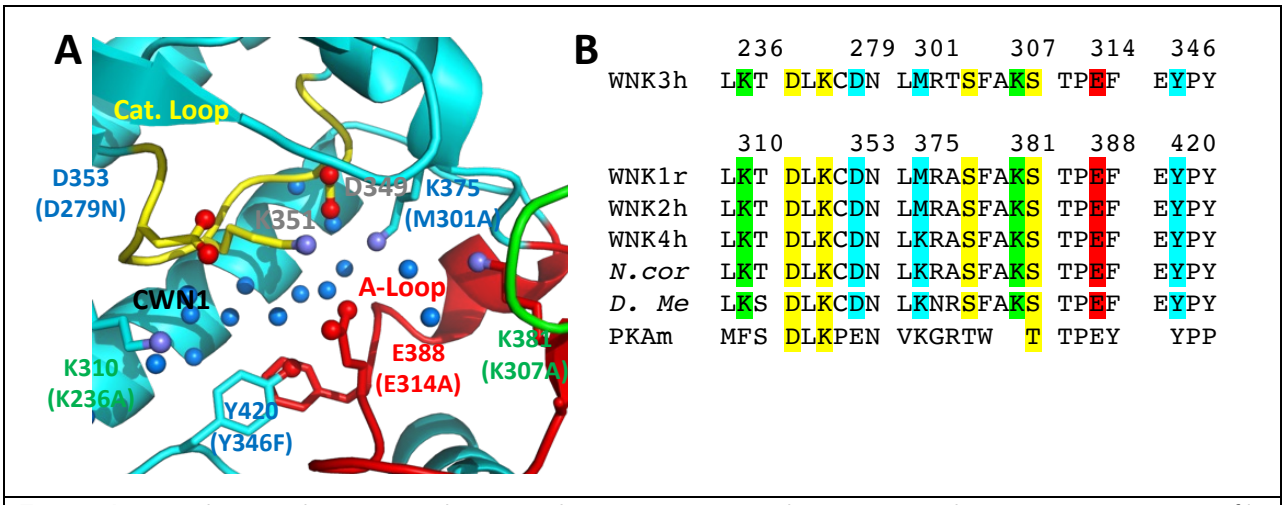

Figure 4. Residues in the AL-CL Cluster and positions mutated. (A) AL-CL Cluster in uWNK1 (PDB file 6CN9). Labels in WNK1 numbering (with WNK3 numbers in parenthesis). Cartoon coloring is the same as Figure 1A. Pan-kinase conserved catalytic residues (D349 and K351) are labelled in gray. AL-CL residue labels are colored to indicate mutant assay results: mutants more active than wild-type, red, similar to wild-type, green, and less active than wild-type, blue. (B) Sequence conservation in the AL-CL Cluster and neighboring residues. Pan-kinase conserved Catalytic Loop residues and pan-WNK Activation Loop phosphorylation sites are yellow, other colors indicate assay results, as in (A).

Expression and phosphorylation state of AL-CL cluster mutants.

Mutational analysis of the AL-CL Cluster was carried out in WNK3. Residues in the Activation Loop, WNK3/E314 (WNK1/388), and K307 (WNK1/381), and a residue in the catalytic loop, WNK3/D279 (WNK1/D353) were mutated. Additional residues that contribute to the ionic AL-CL cluster, K236, M301 (lysine in WNK1) and Y346 were also mutated. AL-CL Cluster mutants were expressed in *E. coli*, purified and the state of

autophosphorylation assessed. Mutant expression levels were variable, but all sufficient to be assayed (Table S3). Activation Loop phosphorylation at WNK3/S308 (WNK1/S382) and WNK3/S304 (WNK1/S378) is necessary for WNK activity (Xu *et al*, 2002). Chymotrypsin-derived peptides were monitored by LC-MS to determine Activation Loop phosphorylation state (Table S4). Each of the mutants were at least 95% phosphorylated as expressed, suggestive of proper folding (Table S3). Mutant proteins were dephosphorylated to form uWNKs (see Methods). Basal autophosphorylation activity of AL-CL mutants was measured under standard conditions (Table S5). A range of phenotypes was observed from more active to less active than wild-type WNK3 (Figure 5 (A-H, purple progress curves)).

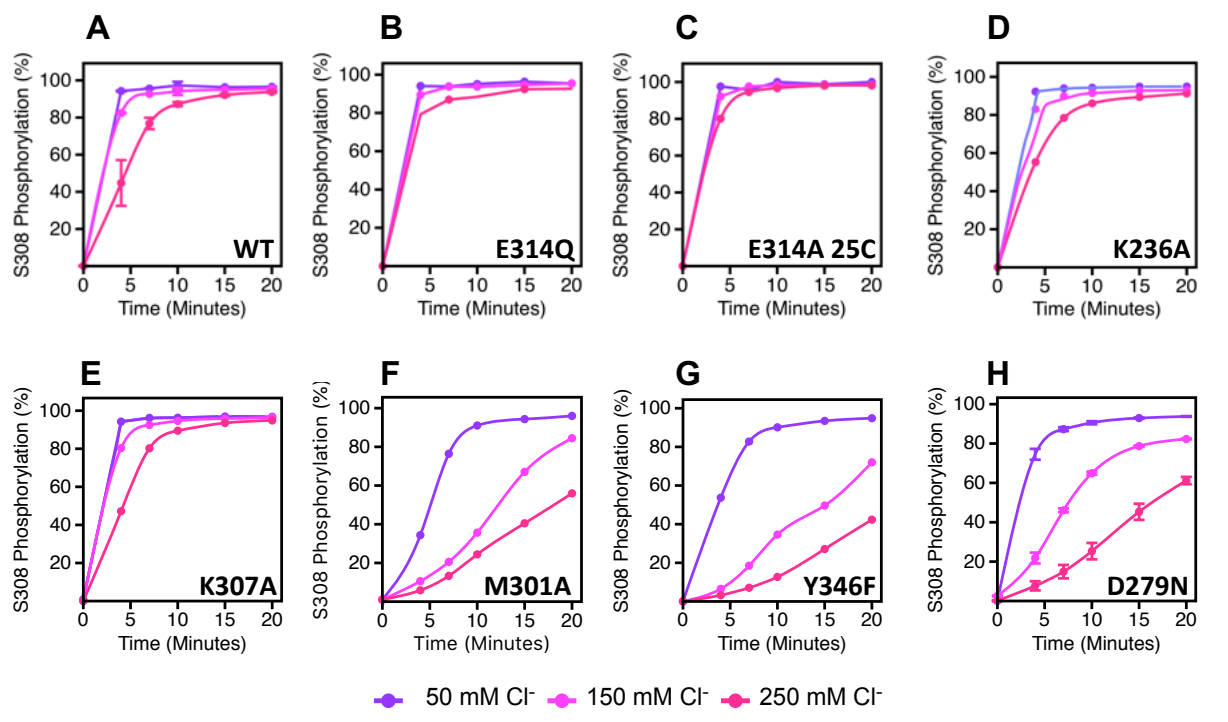

Figure 5. Effects of chloride on uWNK3 AL-CL Cluster mutant autophosphorylation at S308. (A) Wild-type uWNK3 . (B) uWNK3/E314Q. (C) uWNK3/E214A at 25 °C. (D) uWNK3/K236A (E) uWNK3/K307A (F) uWNK3/M301A. (G) uWNK3/Y346F. (H) uWNK3/D279N. Reactions run in 4 μM uWNK3, 30°C (unless otherwise indicated), at chloride concentrations of 50 mM (purple), 150 mM (pink), and 250 mM (magenta). Bars indicate standard error from triplicate independent experiments.

WNK3 AL-CL Cluster mutant chloride sensitivity

Chloride ion exhibits large inhibitory effects on WNKs (Piala *et al.*, 2014). To probe whether AL-CL cluster mutants affect WNK chloride regulation, we measured the chloride inhibition of uWNK3 autophosphorylation. The precise content of the assay buffer is given in Table S5. Assays were run at 4 μM uWNK3. The AL-CL Cluster mutants exhibited three different chloride inhibition phenotypes (Figure 5): (1) more autophosphorylation competent and less sensitive to Cl^-, (2) similar to WT; and (3) less autophosphorylation competent and more sensitive to Cl^-. The mutants WNK3/E314Q and WNK3/E314A were more active than wild-type and exhibit reduced chloride sensitivity (Figure 5B, 5C). WNK3/E314A was assayed at a reduced temperature because of its high activity. Mutation of lysine residues on the periphery of the AL-CL Cluster (K236A and K307A) are little changed from WT (Figures 5D, 5E). K307A has only a small effect, even though it is adjacent to the phosphorylation site at Ser308. Effects of chloride on S304 phosphorylation was also tracked (Figure S1). S304 is typically phosphorylated more slowly than S308. Each of the more active mutant had similar effects on S304 as on S308 (Figure S1).

The mutants WNK3/D279N, M301A and Y314F show related and complex phenotypes. These mutants are less active than WT and much more sensitive to chloride (Figures 5F-H). S304 is phosphorylated more slowly than S308 for both wild type and mutants. In general, the effects of mutation of different sites on phosphorylation of this peptide mirrored the effects on Ser308 phosphorylation: wtWNK3 and WNK3/E314A the most active, K236A and K307A similar to wild-type, and M301A, Y346F and D279N least active. S304 phosphorylation appears to be more sensitive to chloride than S308 phosphorylation in these less active mutants (Figure S1).

WNK3 AL-CL Cluster mutant osmotic sensitivity

The osmolyte PEG400 was used to put a demand on solvent in vitro as a mimic of osmotic pressure effects in cells (Kuznetsova *et al.*, 2014). We previously observed that PEG400 stimulates ATP consumption by WNK3 in the presence of substrate GST-OSR1 (Akella *et al.*, 2021). Unlike the LC-MS method used to study chloride inhibition, ADP-Glo is compatible with PEG400. The high activity mutant WNK3/E314Q, and two less active mutants WNK3/D279N and Y346F were selected for assays (Figure 6). Osmotic effects on WNKs measured in vitro with osmolytes are generally smaller than the chloride effects (Akella *et al.*, 2021; Piala *et al.*, 2014). In this assay, the mutants followed a trend of less activity, with little change in the osmosensitivity. Apparently, none of the single point mutations abolished the osmosensitivity.

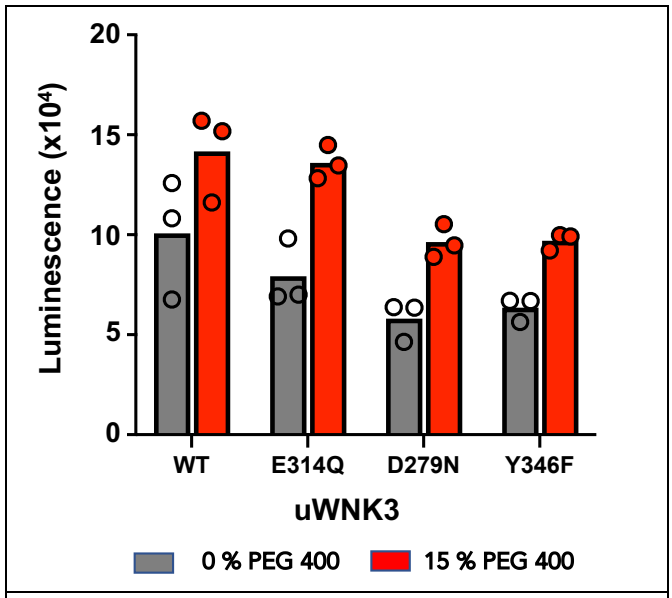

Figure 6. Effects of osmolytes on uWNK3 AL-CL cluster mutants. ADP production is measured by ADP Glo® (Promega) with gOSR1 peptide as a substrate in the absence (grey) or presence (red) of 15% PEG400 15 min, 25°C. Luminescence is proportional to ATP consumption. Circles represent independent triplicated experiments.

The high activity of the mutant WNK3/E314Q and E314A is most easily interpreted as a loss of stability of CWN1-stabilized inhibitory conformation. The lower activity mutants require more data to understand, but all are in the active site, and potentially could affect substrate binding or catalysis.

Static Light Scattering of mutant WNK3

To check whether the mutations effected the oligomeric state, SLS was performed on wt and mutant uWNK3 between 0.8 mg/ml and 2.4 mg/ml at room temperature as described previously (Akella *et al.*, 2021) (Table S6). Based on the 40 kD molecular weight of one subunit of uWNK3, wt uWNK3 is a mixture of monomer and dimer. Two of the mutants behave similar to wild-type including K236A and Y346F. Two other mutants on the Activation Loop are well behaved showing a monomer-dimer mixture at both concentrations (M301A, K307A). Three of the mutants were either aggregated or form higher order oligomers, including E314Q, E314A and D279N. The faster mutants tested at WNK3/E314, despite their enhanced activity, are not monomeric.

DISCUSSION

WNKs are activated in cells both by osmotic stress and low chloride. The osmolyte PEG400, which put a demand on solvent, induced de-dimerization of WNK1/SA in crystals and change in space group. The conformational changes take place in parts of the structure that change shape on activation of WNKs. PEG400 eliminates many of the water molecule observed in CWN1 in the inactive dimer, and all of the waters in CWN2. Apparently, the water networks may be considered allosteric ligands that promote the inactive structure of WNKs. PEG400 also eliminates the binding site for chloride, another inhibitory ligand.

We probed the potential role of CWN1 as an allosteric ligand by mutating residues that stabilize it, the AL-CL Cluster. Changes in autophosphorylation activity and chloride sensitivity were observed. Two hyper-active mutants were discovered, WNK3/E314A, and WNK3/E314Q. These mutants are straightforward to interpret based on our model: the mutated residues support and stabilize inactive dimeric WNK. On the other hand,

proximity of the AL-CL cluster to the active site probably explains the low activity of the slow mutants. However, only small changes in osmolyte activation were seen. We look forward to future data to determine the effects of disrupting other water networks, making multiple mutations, and data on the mechanism of other osmotic pressure sensors to ascertain the generality of the themes observed here.

MATERIALS AND METHODS

Reagents and Clones

Lambda phosphatase was purchased from Santa Cruz Biotechnologies. An expression plasmid encoding PP1cγ was a gift from Dr. Depaoli-Roach (Indiana University) and purified according to (Barford & Keller, 1994) as described previously. Standard reagents for purification and mass spectrometry we purchased from Sigma and Fisher Scientific. DNA human WNK3 (118-409) was subcloned into a pET29b vector by Genscript Inc. (New Jersey) (Akella *et al.*, 2021). Mutants of WNK3 based on the AL-CL Cluster in WNKs were also synthesized by Genescript, Inc. These mutants are WNK3/E314A, K236A, K307A, M301A, Y346A, and D279N (Table S7).

Expression and purification of WNK3 and its mutants

Purification of WNK1 kinase domain for crystallization was performed following protocols in Min, 2004, #4183}. The kinase domain of WNK3 (WNK3(118-409)) expresses well in BL21(DE3) *E. coli* cells. WNK3 and mutants were expressed and purified in pET29b using modifications of the original protocol (Min *et al.*, 2004). Colonies were grown in terrific broth (TB) containing the antibiotics kanamycin and chloramphenicol on an INFORS shaker overnight at 37 °C. 800 µL of cultured cells were transferred to 50 mL of TB at 37 °C and grown to OD_{600} = 1.8; then 16 mL were transferred to 1 L of TB and grown to OD_{600} = 1.3. Protein expression was induced with 0.5 mM isopropyl

thiogalactopyranoside (IPTG). Cultures were grown for 18 h, at 18 °C and 180 rpm. Cells were pelleted by centrifugation and flash frozen in liquid N_2. Cells were lysed in an Avastin cell disruptor, and the lysate ultracentrifuged. The WNK3 was extracted from the supernatant on a $NiSO_4$-charged Sepharose column (GE) which was loaded in 50 mM Tris-HCl pH 8, 500 mM NaCl, 5 mM imidazole and eluted in 250 mM imidazole. After dialysis in 50 mM Tris-HCl pH 8, 50 mM NaCl, 1 mM EDTA, and1 mM dithiothreitol (DTT), the WNK3s were further purified a Mono-Q 10/100 GL column (GE) eluted with 1 M NaCl. Samples were concentrated using an Amicon (Millipore), and buffer exchanged to 50 mM hydroxyethyl piperazine ethanesulfonic acid (HEPES) pH 7.4, 50 mM NaCl, 1 mM EDTA and 1 mM Tris carboxyethyl phosphene (TCEP). The HEPES buffer was made using HEPES free acid (Fisher) and adjusted to pH 7.4 using Tris base (Fisher). Gel filtration was performed on a Superdex-75 16/60 column.

WNK3 is phosphorylated (pWNK3) as purified from *E. coli*. Extent of phosphorylation of the different mutants is in Table S3. Phosphorylated WNK3 (pWNK3) was dephosphorylated using PP1cγ and λ-phosphatase in a 10:1 ratio, in 0.5mM $MnCl_2$. Phosphatases were removed using Ni-NTA and gel filtration chromatography as described (Akella *et al.*, 2021). The uWNK3 was stored in 50 mM HEPES pH 7.4 and 150 mM NaCl.

Crystallization and PEG400 treatment of uWNK1 crystals and x-ray methods

Crystals of WNK1/SA were obtained as reported previously (Akella *et al.*, 2021; Min *et al.*, 2004), grown in 24% PEG 2000, 300 mM NaCl, and 100 mM HEPES, pH 7.5, and cryoprotected in 15% glycerol, 26% PEG2000, and 300 mM NaCl, pH 7.5. Crystals were in space group P1, with cell constants *a*=38.30 Å, *b*=57.8 Å, *c*=65.7 Å, α =91.3°, β=89.99°, γ=90.89°. Recently, we obtained crystals under different condition of reduced chloride containing 200 mM potassium formate and 20% PEG3350. These crystals when

cryoprotected with 15% glycerol diffracted to 2.0 Å. The unit cell dimensions of *a*=38.2 Å, *b*=57.7 Å, *c*=65.6 Å α = 89.0°, β=89.6°, γ=89.2° were similar to that reported earlier (PDB 6CN9). These crystals were then exposed to 25%PEG400 in the same buffer for 25 min to determine the effect of PEG400 on the crystals. The space group changed to $P2_1$ with altered lattice constants, *a*=38.3 Å, *b*=56.8 Å, *c*=65.3 Å, β=95.4° without significant loss of resolution.

Generic assay conditions

Assays were conducted in 20mM HEPES, pH 7.4, 20 mM $MgCl_2$, 5 mM ATP and usually in 150 mM NaCl at room temperature. Reactions were initiated by the addition of uWNK3 or uWNK1 to 4 μM. Substrate phosphorylation assays contained 40 μM gOSR1. Reactions were stopped by addition of guanidine-HCl to 1M. The content of the assay buffer is given in Table S5.

Autophosphorylation of uWNK3 and mutant uWNK3 methods

Chloride sensitivity of in vitro phosphorylation assays were caried out in a water bath at 30 °C, in 20 mM HEPES pH 7.4, 20 mM Mg-gluconate and 5 mM ATP. Varying concentrations NaCl were added to the reaction mix. Chloride inhibition was measured at 50, 150 and 250 mM total Cl^-. Reactions were started by adding 4 μM of uWNK3 or uWNK3 mutant. Aliquots of 50 μL were removed at time points: 0, 4, 10, 15 and 20 min and stopped by addition of guanidine-HCl to 1M. Assay contents in Table S5.

Mass spectrometry methods.

The reaction mixes were diluted with chymotrypsin mix (rendering the solutions 0.5 μM chymotrypsin, pH 8.0, 500 mM guanidine-HCl and 25 mM $CaCl_2$) and incubated overnight at 30°C. Peptide separation and detection by mass spectrometry was carried

out as described previously (Akella *et al.*, 2021) . Briefly, HPLC separation was conducted using an RP-C18 column (Phenomenex Aeris Widepore 150x2.1 mm) with a Shimadzu 10ADvp in line with a Thermo Finnigan LTQ. Phosphorylation ratios for S308 and S304 were obtained by integrating the ion traces corresponding to m/z ranges for Activation Loop peptides. Because mutations were introduced into the Activation Loop, the phosphopeptides changed (see Table S4).

ADP-Glo® Assay Methods

ADP-Glo® reagent (Promega Inc.) was used as a readout for autophosphorylation as described previously (Akella *et al.*, 2021). This reagent is compatible with the high ATP concentrations required for uWNK autophosphorylation assays, and can be used, unlike mass spectrometry, in the presence of PEG400. 50 µL reactions contained 40 mM HEPES (pH 7.4), 10 mM $MgCl_2$, 4 µM pWNK, and 40 µM gOSR1. Final chloride concentration was maintained at 150 mM. The reaction was started by the addition of 5.2 mM ATP. Reactions were stopped after 15 minutes with 50 µL of ADP-Glo® reagent in the presence of 100 nM WNK463 pan WNK inhibitor (Yamada *et al.*, 2016). Manufacturers protocols were followed for the remaining steps of ATP depletion (40 min), conversion of ADP to ATP (1 hour). 100 µL aliquots were transferred to a 96-well plate and centrifuged for 2 min. at 800 rpm. Luminescence was read on a CLARIOstar plate reader and data analyzed using MARS software (both reader and software, BMG Labtech, Ortenberg, GER). Data was further processed using GraphPad-Prism software.

Static Light Scattering methods

SLS was conducted on a Wyatt DynaPro Nanostar DLS, at 25 °C. Samples of uWNK3 were prepared at four concentrations (0.8, 1.2, 1.8 and 2.4 mg/mL) in 50 mM HEPES pH 7.4 and 150 mM NaCl. Samples were centrifuged at 16,100 x g for 10 min to remove

aggregates and particles, before 5 µL were loaded into a quartz cuvette. Light scattering at 90° was monitored until the detector voltage was stable, and then the scattering was monitored for ten times for 5 s, with three replicates. Data were analyzed using Dynamics version 7.5.0.17 (Wyatt Technologies).

Comparing water structure across multple PDB files.

ProBis_H2O (Jukic *et al*, 2017) was used to find clusters of conserved water molecules in the nine WNK1 kinase structures deposited in the PDB The results were manually curated in using PyMOL to compare WNK1 and WNK3 structures and to use local superpositions of domains.

Crystal structure of WNK1/SA in PEG400.

Crystals of WNK1/SA soaked with PEG400 (PEG-uWNK1) exhibited higher symmetry than the uWNK1 crystals (PDB 6CN9). The starting model for molecular replacement was the WNK1/SA (PDB 6CN9). The model was built in COOT based on the |2Fo-Fc| maps. Final restrained refinement containing 250 water molecules against 2.0 Å x-ray data using REFMAC5 in the CCP4 suite for WNK1/SA/PEG400 and including TLS (Translation/Libration/Screw) yielded an R-factor and R-free of 0.20 and 0.23, respectively.

FUNDING

This work was supported the Mary Kay Ash Foundation International Research Scholar Program (LRT), National Institutes of Health (DK110358 to EJG) the Welch Foundation grant I1128 and I-2100-20220331, and CPRIT grant RP190421 to EJG.

ACKNOLWLEDGEMENTS

Results shown in this report were derived from work performed at Argonne National Laboratory, Structural Biology Center (SBC) at the Advanced Photon Source. The SBC is operated by the U Chicago Argonne, LLC, for the U.S. Department of Energy, Office of Biological and Environmental Research under contract DE-AC02-06CH11357. Crystallographic studies were coordinated by Diana Tomchick in the UT Southwestern Structural Biology Laboratory. We thank Chad A. Brautigam and the UTSW Molecular Biophysics Resource Core facility for static light scattering data collection and analysis.

COMPETING INTEREST

The Authors have declared no competing interest.

AUTHOR CONTRIBUTION

LRT obtained the mutant plasmids, expressed and purified the proteins. LRT also performed the autophosphorylation assays of mutants with different chlorides. JMH analyzed the autophosphorylation assays using LC/MS. HH purified proteins, RA and EJG crystallized and analyzed data of PEG400:WNK1 complex. EJG wrote the manuscript and RA, JMH and EJG generated figures.

REFERENCES

Akella R, Drozdz MA, Humphreys JM, Jiou J, Durbacz MZ, Mohammed ZJ, He H, Liwocha J, Sekulski K, Goldsmith EJ (2020) A Phosphorylated Intermediate in the Activation of WNK Kinases. *Biochemistry* 59: 1747-1755

Akella R, Humphreys JM, Sekulski K, He H, Durbacz M, Chakravarthy S, Liwocha J, Mohammed ZJ, Brautigam CA, Goldsmith EJ (2021) Osmosensing by WNK Kinases. *Mol Biol Cell* 32: 1614-1623

Barford D, Keller JC (1994) Co-crystallization of the catalytic subunit of the serine/threonine specific protein phosphatase 1 from human in complex with microcystin LR. *J Mol Biol* 235: 763-766

Goldsmith EJ, Rodan AR (2023) Intracellular Ion Control of WNK Signaling. *Annu Rev Physiol* 85: 383-406

Jukic M, Konc J, Gobec S, Janezic D (2017) Identification of Conserved Water Sites in Protein Structures for Drug Design. *J Chem Inf Model* 57: 3094-3103

Jukic M, Konc J, Janezic D, Bren U (2020) ProBiS H2O MD Approach for Identification of Conserved Water Sites in Protein Structures for Drug Design. *ACS Med Chem Lett* 11: 877-882

Kuznetsova IM, Turoverov KK, Uversky VN (2014) What macromolecular crowding can do to a protein. *International journal of molecular sciences* 15: 23090--23140

Lytle C, Forbush B, 3rd (1992) The Na-K-Cl cotransport protein of shark rectal gland. II. Regulation by direct phosphorylation. *J Biol Chem* 267: 25438-25443

Manning G, Plowman GD, Hunter T, Sudarsanam S (2002) Evolution of protein kinase signaling from yeast to man. *Trends Biochem Sci* 27: 514-520

Min XS, Lee BH, Cobb MH, Goldsmith EJ (2004) Crystal structure of the kinase domain of WNK1, a kinase that causes a hereditary form of hypertension. *Structure* 12: 1303-1311

Piala AT, Moon TM, Akella R, He H, Cobb MH, Goldsmith EJ (2014) Chloride sensing by WNK1 involves inhibition of autophosphorylation. *Sci Signal* 7: ra41

Richardson C, Alessi DR (2008) The regulation of salt transport and blood pressure by the WNK-SPAK/OSR1 signalling pathway. *Journal of Cell Science* 121: 3293-3304

Terker AS, Zhang C, Erspamer KJ, Gamba G, Yang CL, Ellison DH (2016) Unique chloride-sensing properties of WNK4 permit the distal nephron to modulate potassium homeostasis. *Kidney Int* 89: 127-134

Wilson FH, Disse-Nicodeme S, Choate KA, Ishikawa K, Nelson-Williams C, Desitter I, Gunel M, Milford DV, Lipkin GW, Achard JM *et al* (2001) Human hypertension caused by mutations in WNK kinases. *Science* 293: 1107-1112

Xu B, English JM, Wilsbacher JL, Stippec S, Goldsmith EJ, Cobb MH (2000) WNK1, a novel mammalian serine/threonine protein kinase lacking the catalytic lysine in subdomain II. *J Biol Chem* 275: 16795-16801

Xu BE, Min XS, Stippec S, Lee BH, Goldsmith EJ, Cobb MH (2002) Regulation of WNK1 by an autoinhibitory domain and autophosphorylation. *Journal of Biological Chemistry* 277: 48456-48462

Yamada K, Park HM, Rigel DF, DiPetrillo K, Whalen EJ, Anisowicz A, Beil M, Berstler J, Brocklehurst CE, Burdick DA *et al* (2016) Small-molecule WNK inhibition regulates cardiovascular and renal function. *Nat Chem Biol* 12: 896-898

Zheng J, Trafny EA, Knighton DR, Xuong NH, Taylor SS, Ten Eyck LF, Sowadski JM (1993) 2.2 A refined crystal structure of the catalytic subunit of cAMP-dependent protein kinase complexed with MnATP and a peptide inhibitor. *Acta Crystallogr D Biol Crystallogr* 49: 362-365